The use of acoustic emission to investigate fracture process zone in notched concrete beams

H. S. Hadjab[1,*], J.-Fr. Thimus[1] and M. Chabaat[2]

[1]Civil Engineering and Environmental Department, Université catholique de Louvain, Bâtiment Vinci, Place du Levant 1, 1348 Louvain-la-Neuve, Belgium

[2]Civil Engineering Faculty, Université des Sciences et de la Technologie Houari Boumediene, B.P.32, Bab-Ezzouar 16111, Algeria

Acoustic emission (AE) has been used to investigate characteristics of the fracture process zone (length, width and macro crack propagation) in a concrete specimen subjected to four-point bending, using probability and statistical methods. To understand the process of crack growth and fracture, a technique based on AE has been developed. The results are treated according to the laws of probability and statistics. It is shown that these results agree more or less in comparison to those obtained using other techniques.

Keywords: Acoustic emission, concrete, crack propagation, fracture process zone.

LINEAR elastic fracture mechanics predicts that the stress will approach infinity at a crack tip. Since infinite stress cannot be developed in materials, a certain range of inelastic zone must exist at the crack tip. For concrete, this inelastic zone surrounding the crack tip is known as the fracture process zone (FPZ), characterized by complex mechanisms[1–6].

In brittle materials, macro crack growth is associated with a FPZ depending upon the material's microstructure, grain size, rate of loading, dimensions of the specimen and other parameters. The size of the FPZ can be significant[7]. The FPZ can also be the result of micro cracking that occurs in front of the crack tip, somewhat similar to the plastic zone in metals or as the result of nonlinear phenomena existing behind the crack tip such as frictional interlock between tortuous cracked surfaces and discontinuous fractures of unbroken aggregate bridging[8].

Several authors have experimentally investigated the growth of the FPZ. They have shown that its reported nature and exhibited dimensions are significant (Table 1). Such discrepancies probably resulted from differences in observations, specimen geometry and dimensions. The following techniques have been used by the various researchers: (i) Direct – Based on an attempt to observe the material directly: optical microscopy[9], scanning electron microscopy[10,11], and high speed photography[12]. (ii) Indirect – Based on indirect observations: laser speckle interferometry[13], compliance technique[14], penetrating dyes[15], ultrasonic measurement[16], infrared vibro-thermography[17] and acoustic emission technique[18–21].

Since the FPZ is considered as one of the principal mechanisms in the fracture of quasi-brittle materials, the main aim of this study was to obtain more data describing the FPZ characteristics (length, width and macro cracks propagation) using acoustic emission (AE). The interpretation of measurements was done using probability and statistics methods.

Description

Specimen preparation

The specimens were cast in steel moulds of dimensions $60 \times 15 \times 15$ cm according to the recommendations of the ASTM[22]. In order to create a notch, a fine plastic strip of 0.5×3 cm was introduced during casting at the centre and also at the base of the specimens.

The concrete used was composed of CEM I 42.5 R Portland Cement, 0/5 river sand and 7/14 crushed gravel. The mix proportions by weight were 1 : 2 : 3 : 0.5 (cement : aggregates : sand : water). All specimens were stored in an air-conditioned room at 20°C with 90% humidity for 28 days. The average compression strength was about 52 MPa for cubes of $15 \times 15 \times 15$ cm and 15.45 kN for the peak load for tests in a four-point bending (FPB) test.

Tests performed

Twenty-four specimens were tested. Each test consisted of a FPB test with one loading/unloading cycle until 70% of the peak load value (15.45 kN). For each specimen, the accelerometer was made to sweep 6×4 locations (nodes as shown in Figure 1). For each location of the accelerometer, the loading/unloading test (70% of 15.45 kN) was performed. The maximum load capacity of the testing machine was 50 kN; the tests were performed with a displacement control of 0.01 mm/min.

For a better follow-up of the test, a Crack Mouth Opening Displacement (CMOD) was recorded using an extensometer MTS 632.02F-20.

*For correspondence. (e-mail: hadjab@gce.ucl.ac.be)

Table 1. Summary of the fracture process zone (FPZ) sizes

Reference	Specimen type	Specimen dimension l.h.e. (inch)	Notch length (inch)	Material type (c : s : a : w)	Technique used	FPZ length (inch)
13	Notched beams	24 × 5.9 × 1 32.7 × 5.9 × 1.5 32.7 × 5.9 × 2	1 1 1	Concrete 1 : 2 : 2 : 0.5	Laser speckle interferometry	1.57–0.12
6	DCB	22.5 × 27 × 3 15 × 18 × 2.5			Replica technique and optical microscopy	3.4 2.3
14	CT	18 × 9 × 1.5	9	Mortar 1 : 2 : 0 : 0.5	Multicutting technique	1.7
7	CT	20 × 15 × 15 18 × 9 × 1.5	0.4 to 0.6	Mortar 1 : 2 : 0 : 0.5	Scanning electron microscopy	6
18	DCB	136.5 × 42.9 × 11.7	3.9	Concrete 1 : 2 : 3 : 4	Acoustic emission	4
5	CT	8 × 8 × 3.4 17 × 17 × 3.4 25 × 25 × 3.4	4.3 9.2 13.4	Concrete 1 : 2 : 3 : 4	Acoustic emission	0.7 1.5 4.3

DCB, Double cantilever beam; CT, Compact tension specimen.

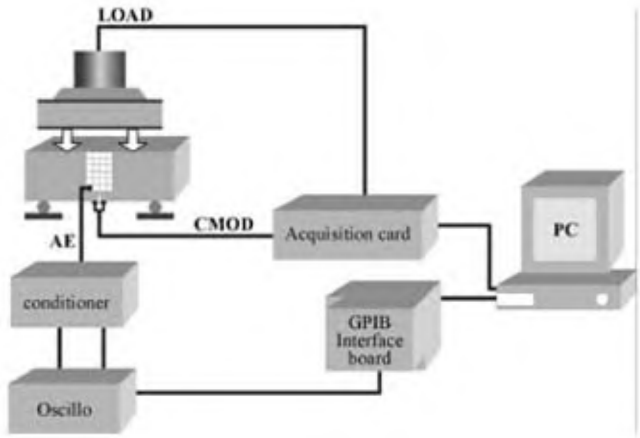

Figure 1. Experimental set-up.

Acoustic emission measurements

An AE is a localized and quick release of strain energy in a stressed material. The released energy causes stress waves, which propagate through the specimen. These waves can be detected at the specimen surface and analysed to evaluate the magnitude and the nature of the damage.

In the case of concrete specimens subjected to a mechanical loading, the AE results from a local fracture. Applications of AE to the detection of cracks and more particularly to the measurement of crack growth have been developed.

The acoustic events were detected by a PCB quartz accelerometer (303 A02), having the following characteristics: resolution 0.01 g (1 ms^{-2} = 0.102 g); sensitivity (nominal) = 10.73 mV/g; resonant frequency 100 kHz, and weight 2.3 × 10^{-3} kg, height 17 mm and diameter 5 mm.

On the basis of earlier results[23], a grid of 20 × 20 mm was designed around the vertical plane of the macro crack. In order to acquire more information about the FPZ during the test, the accelerometer was made to move from node to node and sweep the grid area in a horizontal scanning. For every node in the grid, the AE signals were recorded.

The test measurements and data acquisition were made using the software developed at Civil Engineering and Environmental Laboratory of Catholic University of Louvain, called AUSPICES (Acoustic and UltraSonic Propagation Imaging Complementary to Elapsed Strength).

After amplification and filtration in a conditioner (frequency band from 0.1 to 50 kHz), signals greater than a preset threshold (chosen above the environmental noise) were transformed into impulses and counted. Since many elastic waves can be generated by one event, certain duration was given to each event. That means that even if the threshold is exceeded several times during this time laps, only one event will be counted. The signal of each event can moreover be recorded using an oscilloscope (sampling frequency of 500 Hz) for further analysis. During the test, the noise threshold was fixed at 0.18 g, while the event duration was set to 1 s.

Results

Development and growth of micro cracks in front of the notch of all the tested specimens were monitored to determine the extent of the FPZ in concrete.

Once the specimen was loaded, the AE signals resulting from micro cracking could be detected by the accelerometer mounted on the specimen at different locations of the grid area. The signals were picked up by the data acquisition system. In order to treat the data, which were related to a certain number of random phenomena, including a dispersion of the values, a probability and statistics

approach was used for the 24 tests, one for each specimen. Thus one had to synthesize the observations, test susceptible assumptions causing this dispersion, and finally draw conclusions on the basis of the studied characteristics. Poisson's law tests the probability of mode of fracture. Observation errors were then estimated using a normal law of Gauss for the fields of maximum amplitude average and acceptable approximations were obtained.

Probabilistic and statistical analysis

Using the laws of probability and statistics, the results (amplitude of the AE) were discussed and interpreted in terms of probability. Since the repartition function $F_X(x)$ or frequency of the random variable X is the probability in which the value of X is lower than x, we have the following relation:

$$F_X(x) = P(X < x). \tag{1}$$

According to the probability and statistics approach, a quantile of order q of a random continuous variable X and of a distribution function F_X, is a value u_q defined as follows for a continuous case as:

$$F(u_q) = P(X < u_q) = q. \tag{2}$$

For a discrete case, it is defined by the following relation:

$$x_i < q < x_{i+1} \quad \text{with} \quad F(x_i) < q \quad \text{and} \quad F(x_{i+1}) \geq q. \tag{3}$$

One can define the percentage number as:

$$Q = \frac{100 - u_q}{100}. \tag{4}$$

During the tests, for each of the 24 specimens and for the 6×4 locations of the accelerometer, the amplitudes of the signals of AE were recorded and the maximum amplitudes $Am_{i,j}$ were calculated as follows:

$$Am_{i,,j} = \begin{pmatrix} A_{m_{1,1}} & \cdots & A_{m_{1,24}} \\ \vdots & & \\ A_{m_{24,1}} & \cdots & A_{m_{24,24}} \end{pmatrix}, \tag{5}$$

where i, j denote the specimen number and node location number respectively.

Procedure to estimate the length of FPZ: For a horizontal row formed by four nodes, one calculates the average of maximum amplitudes noted as $\overline{Am}_s$ (where the subscript 's' denotes a given specimen). One obtains six values corresponding to different distances from the macro crack (Table 2).

Procedure to estimate the width of the FPZ: For a given location, the average of maximum amplitudes for the 24 specimens is then noted as $\overline{Am}_j$ If we associate $\overline{Am}_j$ to the continuous random variable X, the percentage event amplitude numbers, A_{q_j}, are equivalent to the quantiles of order q, which has been illustrated in Figure 2 for the 6×4 nodes locations and the 24 specimens. The values of amplitudes present, in terms of statistics, a population verifying Gauss law (see Figure 2) and well-defined by the notion of quantile, which represents the percentage of the amplitude dispersion and are given as:

$$A_{q_j} = \frac{100 - u_q}{100}, \tag{6}$$

where $u_q = \overline{Am}_j$ is the value of the quantile of order q equivalent to $\overline{Am}_j$.

On the basis of A_{q_j} values obtained for each location of the accelerometer, the cumulative average percentage number noted by N was then calculated by summation and average in the same vertical column for all the six values.

Table 2. Accelerometer vertical scanning

Distance from the macro crack, y (cm)	1.0	3.0	5.0	7.0	9.0	11.0
$\overline{Am}_s$ (mV)	8.38	13.44	14.28	15.25	16.51	19.85

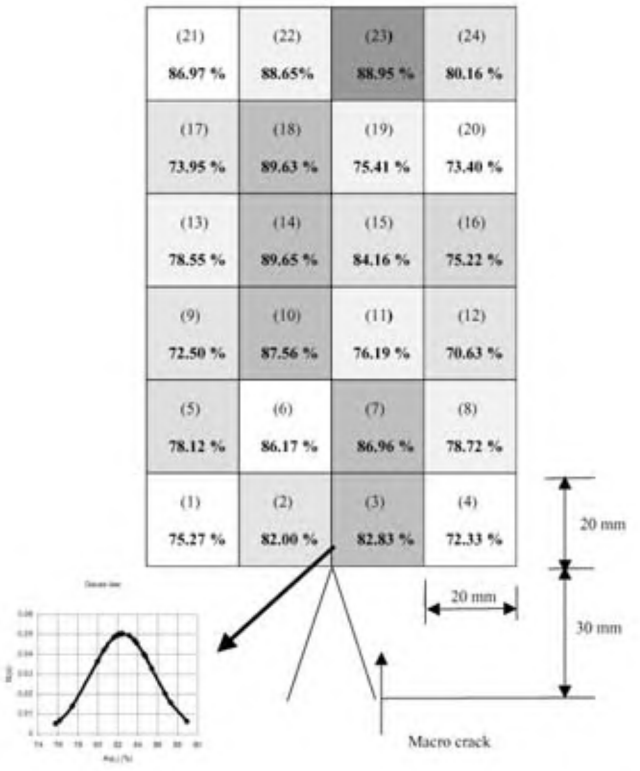

Figure 2. Percentage at the centre of each node, A_{q_j}, where j is the node location number.

Interpretation of results

The probable propagation of the macro crack was then obtained by putting all the results into the grid, and by assuming that the latest (i.e. probable propagation) corresponds to the maximum event percentage (Figure 3). AE enables us to follow the process of propagation of the micro crack in such structures and defines the characteristic of the FPZ by length and width measures.

Discussion

Once the load increases and the main crack propagates, a very long FPL is developed ahead of the macro crack, while the number of AE events progresses dramatically.

Length of FPZ

In the light of the relationship between the average maximum of amplitudes of events ($\overline{Am}_s$) and the distance to the macro crack tip (Figure 4), one can distinguish three regions:

(i) 1.0 cm ≤ y ≤ 3.0 cm – At y = 1.0 cm, $\overline{Am}_s$ is weak and increases from 8.38 to 13.44 mV at y = 3 cm. This may be explained by an intense concentration of the micro crack at the tip of the macro crack (stress singularity). In this region, micro cracks propagate by successions of abrupt jumps and variable speeds (heterogeneity of concrete). Variations in kinetic energy are the result of increasing $\overline{Am}_s$.

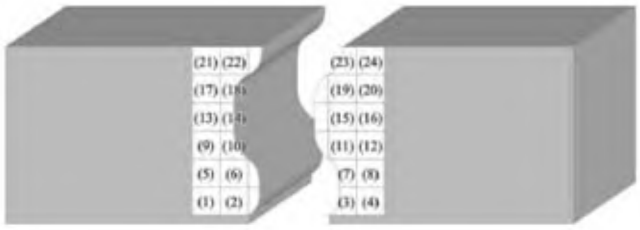

Figure 3. Macro crack propagation.

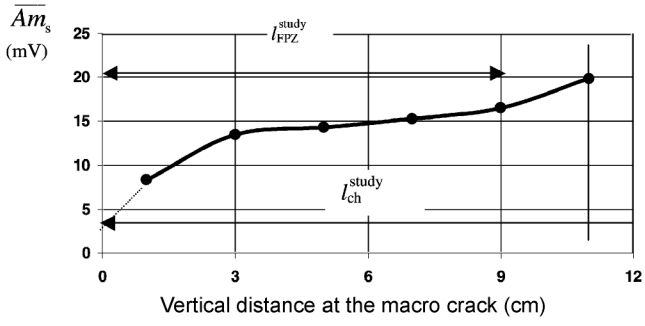

Figure 4. Evaluation of the fraction process zone length.

(ii) 3.0 cm < y ≤ 9.0 cm – $\overline{Am}_s$ increases continuously until a value of 16.51 mV. Here, the small slope in amplitude corresponds to a small decrease in the density of micro cracks. This behaviour can be related to microstructure phenomena.

(iii) y > 9.0 cm – $\overline{Am}_s$ hardly increases until a value of 19.85 mV. This may be explained by hard decreasing in micro cracks.

Figure 5 which presents load and AE events as a function of CMOD, shows four specific zones, that can be described as follows:

Zone 1: In this zone the specimen behaves elastically and one can distinguish two stages:

Stage 1 – It is seen that prior to the point A = 4.10 kN, the CMOD increases linearly until a value of 0.04 mm (Figure 5). The weak AE events indicate that initiation of micro cracks is insignificant. These micro cracks exist due to the younger age of concrete and result from varied shrinkage.

Stage 2 – This stage occurs between points A and B. In this case, the load increases from 4.10 to 6.51 kN. The same increase is observed for AE, as a result of propagation of micro cracks inside the cement matrix.

Zone 2: This zone is represented here between points B and C, and before the peak load. One can see that the curve becomes nonlinear, implying that the CMOD increases from 0.07 to 0.13 mm and the AE events from 390 to 1450. This phenomenon could be explained by the formation of a band of micro cracks, indicating that the damage starts to localize. The macro crack extends slightly before reaching the peak load, creating the so-called FPZ.

Zone 3: In this zone, the load decreases when CMOD increases hardly (from 0.13 to 0.42 mm), but on the other hand, the AE events are steady. Formation of the micro cracks in this zone is stopped, while the macro cracks extend slightly.

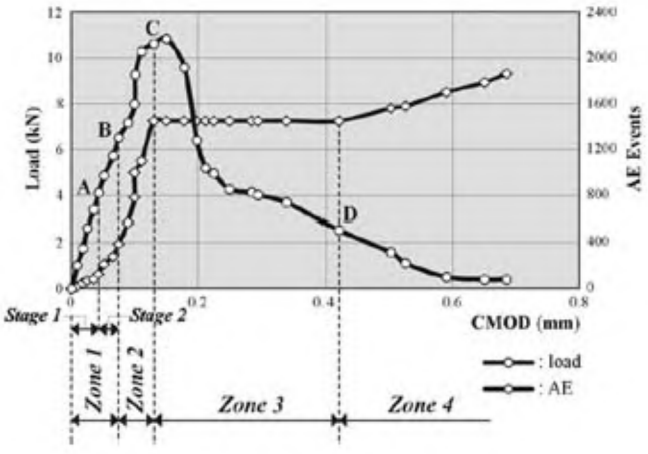

Figure 5. Relation between load, acoustic emission (AE) and crack mouth opening displacement (CMOD).

Zone 4: After the point D, the AE events increase, due to the existence of fracture of the matter's bridges inside the FPZ.

In summary, evolution of the AE events permits one to visualize the micro cracking zone as well as its characteristics. The first micro crack appears at the point B (42% of the peak load). At this point, a continuous zone is formed by numerous micro cracks as defined in zone 2. The relationship between the applied load and the CMOD in a FPB specimen allows us to deduce that one can divide the curve into four zones based on initiation and propagation of the micro cracks. In order to study the FPZ, it is important to know what really happens in this zone. This zone is delimited by two points B and C (about 68% of the peak load). While micro cracks start to localize ahead of the macro crack, propagation of this latest crack begins in proportion to an increase in the load. This phenomenon is found to damage localization or strain localization characterizing the FPZ. On the basis of the results shown in Figure 5, one can conclude that the FPZ length is limited between the point B and just before the peak load.

Figure 4 shows that using the AE events and precisely from 1 cm until 9 cm (vertical distance at the macro crack), the amplitudes increase by the formation of small micro cracks, which may be considered as constant (the uncertainty interval between two successive values is relatively constant in the two first intervals, compared to the third one). In this case, the FPZ extends across the two first intervals represented above and its length has been estimated at a distance less than 9 cm.

Width of FPZ

Figure 6 shows the method developed for measuring width of the FPZ. This can be obtained while drawing the function $N = f(x)$, where N is the cumulated average percentage of events for each vertical node and x is taken as the horizontal distance from the macro crack.

Figure 6 represents a curve with a highest value at the point with coordinates (–1.0, 87.30%) and lowest value at the point with coordinates (3.0, 75.84%). One may divide this curve into two areas:

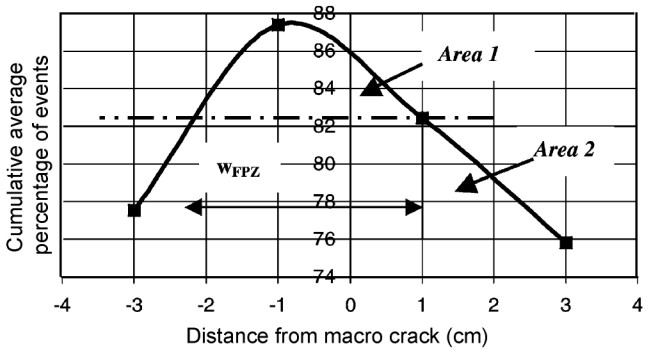

Figure 6. Evaluation of FPZ width.

Area 1 is limited by the more emissive vertical line (87.30%) and the second emissive line (82.42%). This area extends over a width of 3.3 cm. Its width defines a zone of confidence of events in which the amplitudes of AE have low values, which are related to damage of the material. Therefore, the width of this zone corresponds to the so-called security value of a damaged zone occurring in front of the macro crack.

Area 2 is located below the second emissive line and is represented by a lower percentage, which corresponds to larger amplitudes.

If we adopt an arbitrary criterion that allows us to link to a notion of damage, one considers that a vertical line is damaged if it contains more average percentages of events than the horizontal line dividing the curve into two areas. It is important to remark that this line (N = 82.42%) gives us the width of the FPZ at the confidence interval, implying that the width of the FPZ is estimated at 3.3 cm. This is considered to represent 2.75 times larger than the largest one in homogeneity of the structure (aggregate size).

Comparison with other approaches

On the basis of these results, a comparative study with theoretical models taking into account the characteristics of the FPZ was performed. These models were based on Dugdale–Barenblatt energy dissipation mechanism, crack band model by Bazant[3], and fictitious crack model suggested by Hillerborg *et al.*[24].

Bazant modelled the FPZ as a band of uniformly and continuously distributed micro cracks with a fixed width, h_c, as follows:

$$h_c = n_a d_a, \tag{7}$$

where d_a is the maximum aggregate size and n_a is an empirical constant, equal to 3 for concrete. In this work, an approximate average value has been obtained (2.75, as explained above).

For the model by Hillerborg *et al.*, the length of the FPZ is related to the length of the cohesive process zone, which is a purely material property. This is called the characteristic length and is related to the FPZ length. It is calculated using the following relation:

$$l_{ch} = \frac{EG_F}{f_t^2}, \tag{8}$$

where f_t, E and G_F are respectively, the material tensile strength, modulus of elasticity and fracture energy.

On the basis of eq. (8), l_{ch}^{study} is equal to 11.04 cm (E = 37.2 MPa, G_f = 70.1 N/m and f_t = 4.86 MPa).

Hillerborg *et al.* found that in concrete specimens subjected to uniaxial tension, the characteristic length was proportional to the length of the FPZ based on the ficti-

tious crack model. The value of l_{ch} for concrete approximately ranges from 10 to 40 cm.

According to the AE results of our study (Figure 4), the value of FPZ length can be considered as 9 cm (two first intervals represented above).

$$l_{FPZ}^{study} \approx 0.82 l_{ch}^{study}. \quad (9)$$

In this study, the length and width of the FPZ were estimated to be $0.82l_{ch}$ and $2.75d_{agg}$ respectively.

Conclusion

Analyses of the load–CMOD and AE curves implied that macro cracks extend slightly before the load reaches its peak, creating in this way the FPZ. The presence of this zone resulted in stable crack growth before the peak load and was also the main factor responsible for the quasi-brittle fracture response of concrete beyond the peak load. The behaviour of concrete was greatly influenced by the FPZ. To accurately quantify FPZ in concrete, it is important to determine experimentally its dimensions (width and length) as well as the propagation of the macro crack, which are considered important parameters to understand the quasi-brittle fracture phenomenon of concrete.

Interpretation of the results in this study as well as the investigation of measurements by AE enable us to obtain qualitative information. From our point of view, this method does not lay out any rigorous and objective criterion, allowing us by stating from an uncertain number of acoustic events localized in the plan to determine, with a certain precision, the dimensions of the FPZ. In this study, we have used a qualitative approach, taking into consideration only information obtained during the various tests. These results have shown more or less good agreement in comparison with those obtained using other techniques.

1. Shah, S. P., Swartz, S. E. and Ouyang, C., *Fracture Mechanics of Concrete*, John Wiley, 1995, pp. 88–161.
2. Guo, Z. K. and Kobayashi, A. S., Further studies on fracture process zone for mode I: Concrete fracture. *Eng. Fract. Mech.*, 1993, **46**, 1041–1049.
3. Bazant, Z. P. and Kazemi, M. T., Determination of fracture energy process zone length and brittleness number from size effect with application to rock and concrete. *Int. J. Fract.*, 1990, **44**, 111–131.
4. Hadjab, H., Thimus, J.-Fr. and Chabaat, M., Stress analysis: Experimental investigation and mathematical modelling. In MMC 2001, poster. 244, San Diego, USA.
5. Ostuka, K. and Date, H., Fracture process zone in concrete tension specimen. *Eng. Fract. Mech.*, 2000, **65**, 111–131.
6. Chao, K. K., Kobayashi, A. S., Hawkins, N. M., Barker, D. B. and Jeang, F. L., Fracture process zone of concrete cracks. *J. Eng. Mech. ASCE*, 1984, **110**, 1174–1184.
7. Opara, N. K., Fracture process zone presence and behavior in mortar specimens. *Am. Concr. Inst. Mater. J.*, 1993, **90**, 618–626.
8. Van Mier, J. G. M., Mode I fracture of concrete: Discontinuous crack growth and crack interface grain bridging. *Cem. Concr. Res.*, 1991, **21**, 1–15.
9. Derucher, K. N., Application of the scanning electron microscope to fracture studies of concrete. *Build. Environ.*, 1978, **13**, 135–141.
10. Mindess, S. and Diamond, S. A., Preliminary SEM study of crack propagation in mortar. *Cem. Concr. Res.*, 1980, **10**, 509–519.
11. Mindess, S. and Diamond, S. A., Device for direct observation of cracking of cement paste or mortar under compressive loading within a scanning electron microscope. *Cem. Concr. Res.*, 1982, **12**, 569–576.
12. Bhargava, J. and Rehnström, A., High speed photography for fracture studies of concrete. *Cem. Concr. Res.*, 1975, **5**, 239–248.
13. Ansari, F., Mechanism of microcrack formation in concrete. *Am. Concr. Inst., Mater. J.*, 1989, **41**, 459–464.
14. Hu, X. Z. and Wittmann, F. H., Experimental method to determine extension of fracture process zone. *J. Mater. Civ. Eng.*, 1990, **2**, 459–464.
15. Lee, N. K., Mayfield, B. and Snell, C., Detecting the progress of internal cracks in concrete by using embedded graphite rods. *Mag. Concr. Res.*, 1981, **116**, 180–183.
16. Sakata, Y. and Ohtsu, M., Crack evaluation in concrete members based on ultrasonic spectroscopy. *Am. Concr. Inst. Mater. J.*, 1995, **71**, 686–698.
17. Dhir, R. K. and Sangha, C. M., Development and propagation of microcracks in plain concrete. *Matér. Constr.*, 1974, **37**, 17–23.
18. Rossi, P., Fissuration du béton: Du matériau à la structure; application de la mécanique linéaire de la rupture, Rapport de Recherche. 1988 LPC N°150.
19. Maji, A. and Shah, S. P., Process zone and acoustic-emission measurements in concrete. *Exp. Mech.*, 1988, **28**, 27–34.
20. Maji, A., Ouyang, C. and Shah, S. P., Fracture mechanisms of concrete based on acoustic emission. *J. Mater. Res.*, 1990, **5**, 206–217.
21. Ouyang, C., Landis, E. and Shah, S. P., Damage assessment in concrete using quantitative acoustic emission. *J. Eng. Mech.*, 1991, **117**, 2681–2698.
22. ASTM C78-94, Standard test method for flexural strength of concrete, 1994.
23. Hadjab, H., Thimus, J.-Fr. and Chabaat, M., Experimental determination of fracture process zone in concrete using ultrasonics. Rapport interne. 2000, UCL, Belgium.
24. Hillerborg, A., Modéer, M. and Petersson, P. E., Analysis of crack formation and crack growth in concrete by means of fracture mechanics and finite elements. *Cem. Concr. Res.*, 1976, **6**, 773–782.

ACKNOWLEDGEMENTS. We are grateful to the Civil Engineering and Environmental Laboratory, Catholic University of Louvain. The first author was funded by the Commission Internationale pour la Coopération au Développement of the Catholic University of Louvain.

Received 4 October 2005; revised accepted 8 May 2007